



# Multi-Level Detachment Deformation of the West Segment of the South Dabashan Fold-and-Thrust Belt, South China: Insights From Seismic-Reflection Profiling

Hanyu Huang<sup>1,2</sup>, Qinghua Mei<sup>3</sup>, Dengfa He<sup>1\*</sup>, Renqi Lu<sup>2</sup> and Yingqiang Li<sup>4</sup>

<sup>1</sup> School of Energy Resources, China University of Geosciences, Beijing, China, <sup>2</sup> State Key Laboratory of Earthquake Dynamics, Institute of Geology, China Earthquake Administration, Beijing, China, <sup>3</sup> Exploration Branch, SINOPEC, Chengdu, China, <sup>4</sup> SINOPEC Exploration and Production Research Institute, Beijing, China

## OPEN ACCESS

### Edited by:

Yosuke Aoki,  
The University of Tokyo, Japan

### Reviewed by:

Craig Magee,  
University of Leeds, United Kingdom  
Gianluca Vignaroli,  
University of Bologna, Italy

### \*Correspondence:

Dengfa He  
hedengfa282@263.net

### Specialty section:

This article was submitted to  
Structural Geology and Tectonics,  
a section of the journal  
Frontiers in Earth Science

**Received:** 26 November 2020

**Accepted:** 23 April 2021

**Published:** 24 May 2021

### Citation:

Huang H, Mei Q, He D, Lu R and Li Y  
(2021) Multi-Level Detachment  
Deformation of the West Segment of  
the South Dabashan Fold-and-Thrust  
Belt, South China: Insights From  
Seismic-Reflection Profiling.  
*Front. Earth Sci.* 9:633816.  
doi: 10.3389/feart.2021.633816

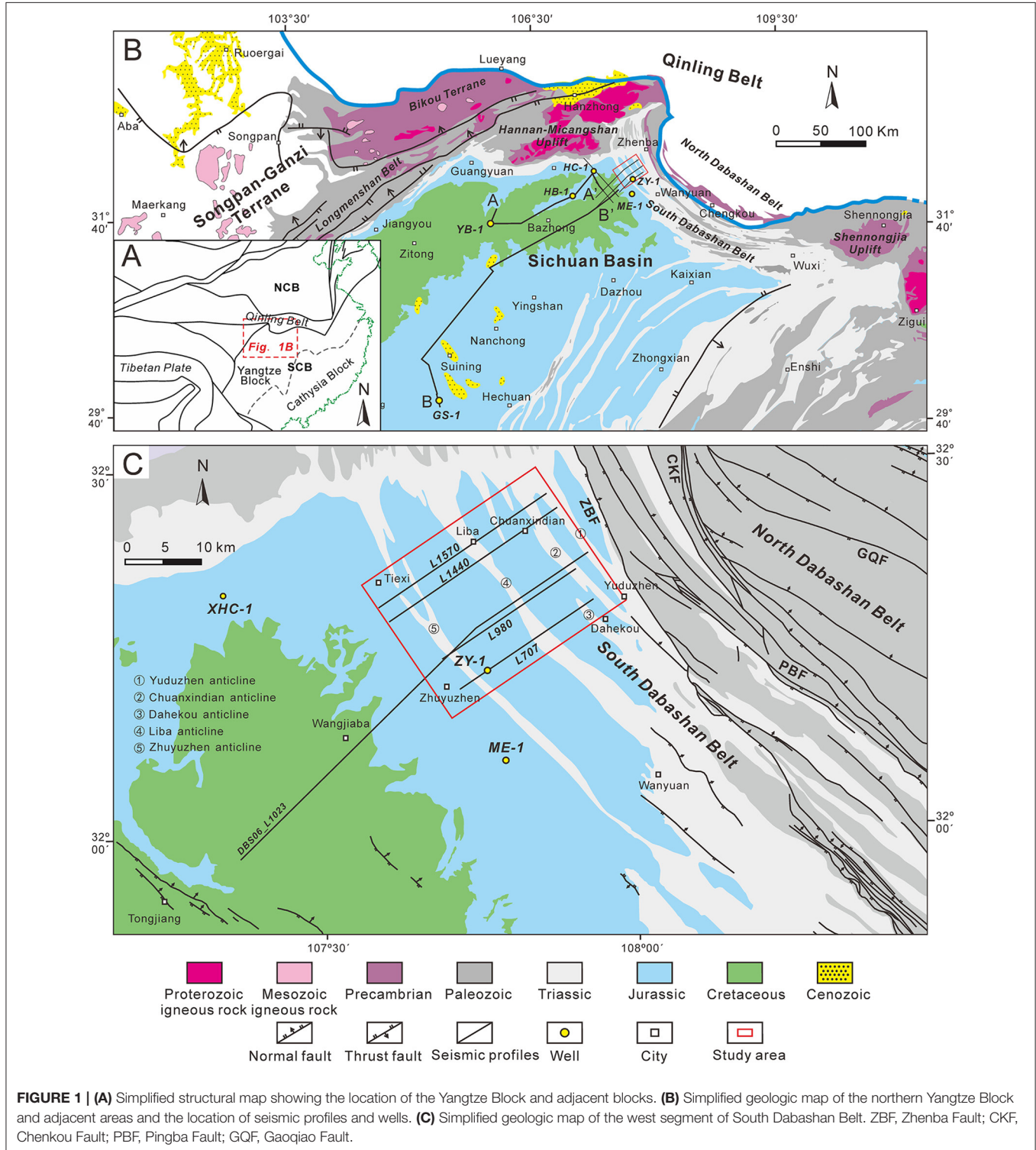
The South Dabashan arcuate tectonic belt located at the northern margin of the Yangtze Block in South China, which primarily comprises a series of northwestern (NW)-trending foreland fold-and-thrust belts (FTBs), is useful for determining the intracontinental orogeny processes of the Yangtze Block. In this study, we integrated the latest pre-stack depth migration of three- and two-dimensional seismic profiles, drill hole, and outcrop data to explore the structural geometric and kinematic features of the west segment of the South Dabashan FTB. This belt is characterized by multi-level detachment structures due to the presence of three predominant sets of weak layers: the Lower Triassic Jialingjiang Formation gypsum interval, Silurian mudstone beds, and Cambrian shale beds. The belt is accordingly subdivided vertically into three structural deformation systems. The upper system appears above the Jialingjiang Formation gypsum layer and exhibits Jura-type folds, which were formed by alternating anticlines and synclines that are parallel to each other. The middle system comprises Silurian shale as the base and Jialingjiang Formation gypsum interval as the passive roof and exhibits NW-striking imbricate thrusts. The lower system is bounded by Cambrian and Silurian detachment layers, forming a duplex structure. The Sinian and Proterozoic basements below the Cambrian were not involved in deformation. The west segment of the South Dabashan FTB underwent four periods of tectonic evolution: Late Jurassic to Early Cretaceous, Late Cretaceous, Paleogene, and Neogene to Quaternary. The deformation was propagated southward in imbricate style, resulting in the passive uplifting of the overlying strata. Based on the magnetotelluric and deep seismic profile, the tectonic processes of the west segment of the South Dabashan FTB are inferred to be primarily controlled by the Yangtze Block northward subduction under the Qinling Orogenic Belt and the pro-wedge multi-level thrusting during the Late Jurassic to Cretaceous.

**Keywords:** Yangtze Block, Dabashan belt, seismic interpretation, detachment layer, intracontinental orogeny

## INTRODUCTION

The Dabashan arcuate orogenic belt is located in the transitional zone between the Yangtze Block (YZB) and the Qinling Belt, China (Figure 1C), and was thought to be related to the

convergence of North and South China Block, after the closure of the Paleo-Tethys since the Triassic (Dong et al., 2013). The Dabashan belt comprises the North and South Dabashan Belts, which are separated by the Chengkou Fault (CKF) (Figure 1C). In the North Dabashan Belt, the passive continental margin



sedimentary cover along the northern YZB (Liu and Zhang, 1999; Lai et al., 2000, 2004; Dong et al., 2008, 2012) is arranged to form a series of thrust nappes during the convergence of the South China Block (SCB) and North China Block (NCB) since the middle Triassic (Xu et al., 1986; Meng and Zhang, 1999; Xiao et al., 2011; Shi et al., 2012). The South Dabashan Belt is far from the plate margin and was considered as a fold-and-thrust belt formed as a product of intracontinental deformation since the Late Jurassic (Liu et al., 2005; Wang et al., 2006; Li and Ding, 2007). Recent studies combined low-temperature thermochronology and provenance analysis of the Sichuan Basin to demonstrate that the South Dabashan Belt experienced multi-stage superimposed deformation and finally formed in Cenozoic (Shen et al., 2007, 2008; Cheng and Yang, 2009; Li J. et al., 2010, 2018; Xu et al., 2010; Yang et al., 2017).

Mesozoic to Cenozoic strata are widely exposed in the western section of the South Dabashan Belt, and the attractive Jura-style fold and thrust belt is preserved. Thus, the west segment of the South Dabashan FTB is an ideal location to study the intraplate deformation feature and its deformation mechanism. In addition, the South Dabashan FTB has gradually become an important oil and gas exploration field, which has increased the research interest of oil and gas explorers. The structural style (Meng and Zhang, 2000; Li et al., 2006; Deng et al., 2010; Zhang et al., 2010; Dong et al., 2011), formation mechanism (He et al., 1997; Wang et al., 2005; Shi et al., 2012; Liu et al., 2015), and thermochronological analysis (Ratschbacher et al., 2003; Li J. et al., 2010; Li P. Y. et al., 2010; Xu et al., 2010; Yang et al., 2017) of the South Dabashan FTB have been studied previously, and the studies concluded that the South Dabashan FTB is a product of the intracontinental thrusting propagation orogeny since the Mesozoic. However, most structural models were based on inferences from field profiles and lacked accurate descriptions of complex underground structures, which limits the accuracy of the current discussion on the evolutionary processes and deformation mechanisms of the South Dabashan FTB. Recently, the Sinopec Exploration Southern Company has collected three-dimensional (3D) and two-dimensional (2D) seismic data in the west segment of the South Dabashan FTB, combining drilling and logging data to form synthetic records that can combine seismic profiles with geological stratification, and image the subsurface structure. This process improves the accuracy of the depiction and elucidation of the structural geometry of this area. Moreover, substantial magnetotelluric data in this area provide deeper structural information for discussing the deformation mechanism.

The present study presents high-quality seismic data with a detailed structural interpretation. We also analyzed the balanced geological cross section and performed kinematic reconstruction of the west segment of the South Dabashan FTB, based on 2D and 3D seismic interpretations and previous related studies. Finally, we use our results to discuss the intraplate tectonic deformation mechanism of the South Dabashan Belt and attempted to reveal the tectonic processes of NCB colliding with YZB based on a combination of magnetotelluric and deep seismic data.

## GEOLOGIC SETTING

The South Dabashan FTB is separated from the North Dabashan Belt by the arcuate CKF to the north (**Figure 1C**) and is adjacent to the Sichuan Basin to the south, the Micangshan–Hannan Uplift to the Northwest and the Shennongjia Uplift to the Southeast, with a general trend NW–SE. The belt presents an arcuate geometry bulging southwestward (**Figure 1B**). Based on the deformation intensity, deformation pattern, and structural trend, the South Dabashan Belt can be divided into three segments: the west, middle, and east segments. The west segment of the South Dabashan FTB is N–S to NNW–SSE trending, and the basement detachment zone is composed of overthrust nappe; the middle segment is NW–SE trending, and is parallel to the North Dabashan Belt; and the east segment is nearly W–E trending, showing evident differences in structural deformation patterns, with a wide exposure of a basement detachment zone, and a tightly folded Paleozoic strata. The study area is located in the west segment of the South Dabashan Belt and exhibits the typical characteristics of Jura-type folds with narrow anticline and broad syncline. In the study area, the South Dabashan Jura-type fold belts mainly comprise Yuduzhen, Chuanxindian, Dahekou, Liba, and Zhuyuzhen anticlines with the Middle–Lower Triassic and Jurassic strata exposed, while the Wangjiaba low amplitude fold belt in the northern Sichuan Basin primarily has exposed Cretaceous strata (**Figure 1C**).

The Sichuan Basin, located in the Upper YZB, essentially completed its current structural framework in the Cenozoic (Huang et al., 2020), and is composed of marine and terrestrial sedimentary rocks on a Precambrian crystalline basement (Huang et al., 2018; Li Y. et al., 2018). The stratigraphic units in the South Dabashan FTB are similar to those in the Sichuan Basin, primarily comprising a succession of marine sedimentary sequences from Sinian to Middle Triassic formed in the margin of the intracratonic basin, and terrestrial sedimentary sequences developed from the Late Triassic to Neogene in the foreland basin, mainly composed of Sinian (100–700 m, shale and carbonate rocks), Cambrian (1,500–2,500 m, mainly shale and carbonate rocks), Ordovician (100–500 m, sandstone, shale, and carbonate rocks), Silurian (0–1,800 m, shale and mudstone), Permian (110–890 m, mainly carbonate rocks), Triassic (1,200–3,300 m, sandstone, evaporates, and carbonate rocks), Jurassic (0–4,900 m, mainly sandstone and mudstone), and Cretaceous (0–1,130 m, mainly sandstone and mudstone). Due to the collision of the YZB and NCB during the late Indosinian period ( $T_3-J_1$ ), the first phase of thrust nappe occurred in the North Dabashan Belt. In the Middle Yanshanian period ( $J_3-K_1$ ), the second phase of intense thrust nappe took place, and the North Dabashan Belt was further folded and deformed, and the regional extrusion stress was transferred to the southwest, leading to the thrust fault-related fold deformation of the initial South Dabashan Belt. In the late Cretaceous, the Dabashan area comprehensively moved into the uplift and denudation stage, and tectonic activity was relatively calm. During the Eocene and Oligocene, the Dabashan Belt became active again due to the far-field efficiency of plate collision of the India and Qinghai–Tibet blocks. After the Miocene, rapid uplift denudation occurred in

the South Dabashan Belt; the strata were denuded and finally formed the present geomorphological condition.

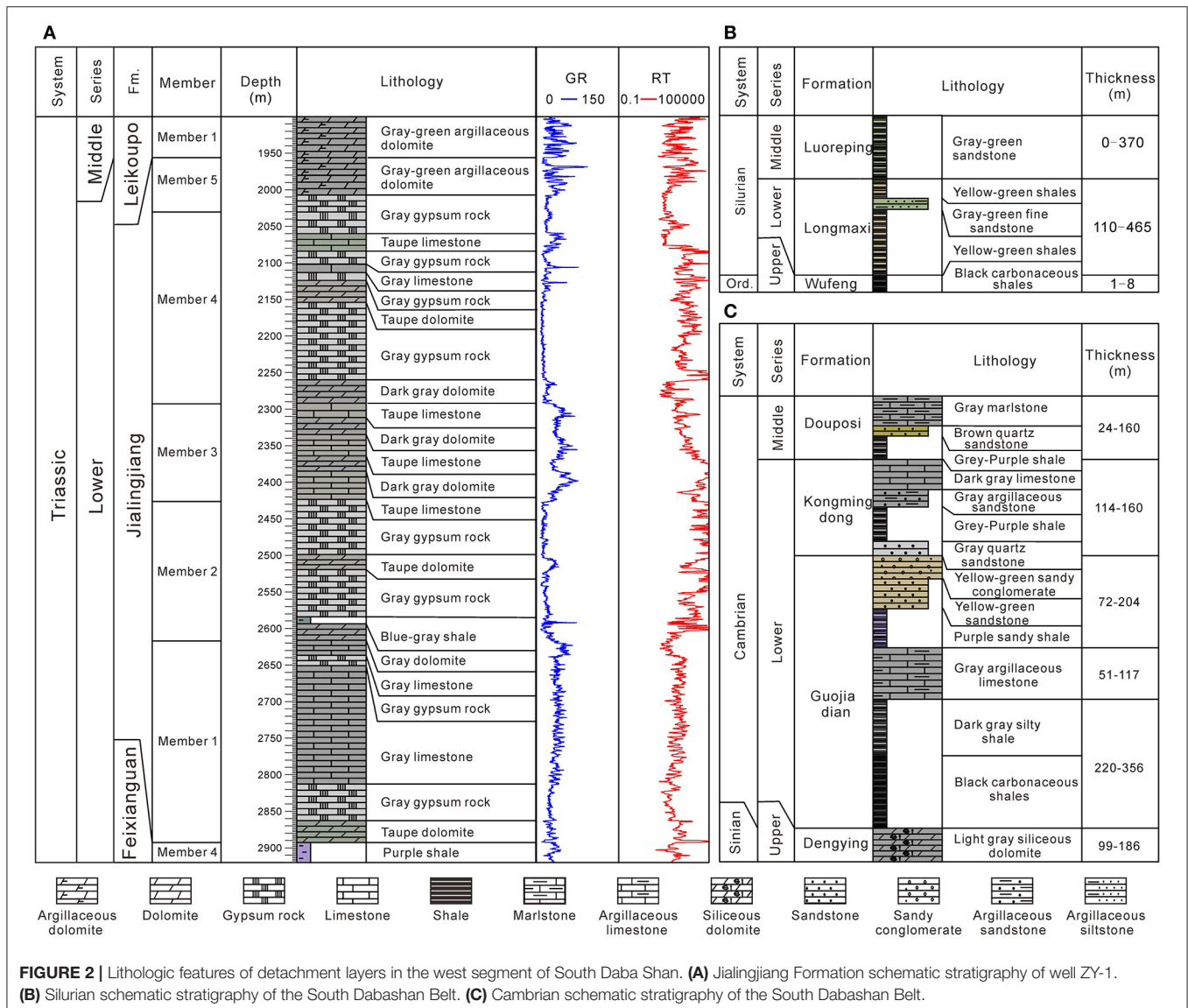
### DATA AND METHODS

Comprehensive seismic data on the west segment of the South Dabashan FTB forms the foundation for the study of its structural geometric features. We predominantly used 2D and 3D seismic profiles, and drill core and outcrop data from the west segment of the South Dabashan FTB. Some 2D seismic reflection profiles and drill data in the northern Sichuan Basin were also used to compare seismic horizons, and finally, magnetotelluric data across the Dabashan area was used to describe the deeper structure. This study uses a 320 km<sup>2</sup>, high-quality prestack time-migrated 3D seismic reflection survey, which has a line spacing of 20 m and a vertical resolution of ~25–50 m (based on an interval velocity of 6,000 m/s, and peak frequency of 30 Hz) at the interval

of interest. Seismic reflection data were then depth-converted using an average velocity of 6,000 m/s.

The synthetic seismograms of wells ZY-1 and HB-1 were used to calibrate the seismic horizons of the study area. Additionally, the long 2D seismic profiles across the South Dabashan Belt and Sichuan Basin were used to trace the seismic horizons of the South Dabashan Belt as the seismic event is continuous in the Sichuan Basin. In addition, due to the complexity of the surface of South Dabashan (which is characterized by rugged topography, changeable lithology of outcrop, and steep strata), the reflection horizon at the shallow part and the edge of the seismic profile would be distortion. Therefore, in the process of interpreting seismic reflection profiles, we used 1:200,000 regional geological mapping results and projected them onto seismic profiles to constrain the underground structural model.

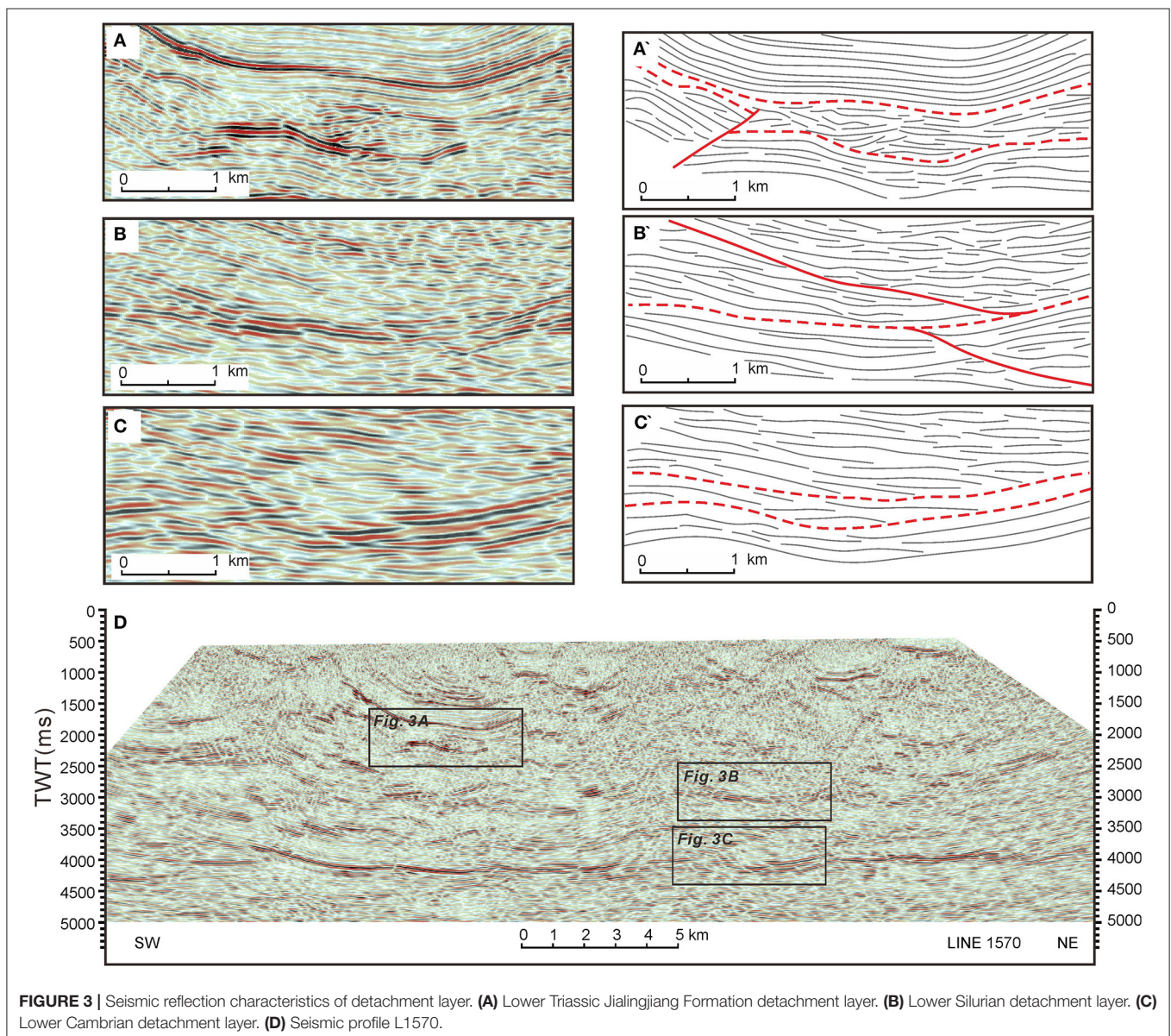
The well ZY-1, located on the northeast wing of the Zhuyuzhen anticline, was eventually drilled into the Upper



Permian strata and was primarily used to calibrate the seismic horizon above the Upper Permian (**Supplementary Figure 1**). The Late Permian and substrata were defined by synthetic seismographs from deep wells (i.e., HB-1 and GS-1) in the adjacent Sichuan Basin, which were extended to the Southern Dabashan area by continuous tracing of the horizon (**Supplementary Figure 2**). The synthetic seismogram of well ZY-1 was obtained based on the well log and drill core data, and the following marker beds were identified: the black shale at the bottom of the Xujiahe Formation ( $T_{3x}$ ) makes unconformable contact with the lower Leikoupo Formation ( $T_{2l}$ ), characterized by strong amplitude, and is one of the main marker beds in the study area. The Jialingjiang Formation Member IV ( $T_{1j}^4$ ) and Member II ( $T_{1j}^2$ ) are 262.5 and 191 m thick, respectively, and primarily comprise of gypsum, intercalated by dolomite and

limestone. Both the  $T_{1j}^4$  and the  $T_{1j}^2$  are moderate amplitudes in the synthetic seismogram and are important detachment layers of the area. The gypsum interval is characterized by chaotic reflection in the seismic profile whose thickness varies significantly. The bottom of the Jialingjiang Formation ( $T_{1j}$ ) comes into contact with the lower Feixianguan Formation characterized by relatively weak amplitude in the synthetic seismogram (**Supplementary Figure 1**).

The synthetic seismograms of wells HB-1 and GS-1 in the Sichuan Basin showed strong amplitude between the Upper and Middle Permian, which may serve as an important regional marker bed. Seismic waves are characterized by moderate amplitude as it spans from the low-velocity layer of the Lower Cambrian's Qiongzhusi Formation mudstone to a high-velocity layer of the Upper Sinian's dolomite, and can be traced and



correlated to the west segment of the South Dabashan FTB (**Supplementary Figure 1**).

The detachment layer is usually characterized by low compressive strength and density, low viscosity, and ample water (Dean et al., 2015; Morley et al., 2018). For a deformation system containing only a single set of detachment layer, the strata above the detachment layer deforms strongly, and thrust faults are often developed, and the strata below the detachment layer are often weakly deformed. For a deformation system with multiple sets of detachment layers, faults are often truncated vertically by detachment layers and by bedding detachment beds, and the patterns of faults developed above and below the detachment layer are often different. Additionally, the low-seismic velocity, low resistivity, and high-conductivity features of detachment layers make their identification clear.

As the thickness of most strata in the study area remains relatively stable, we selected the undeformed strata in the foreland area as the nail point and used the line length conservation principle to restore the 2D geological profile. In addition, for the gypsum and mudstone detachment layers with strong deformation, we restored them based on the area conservation principle (Dahlstrom, 1969; Geiser, 1988).

## STRUCTURAL GEOMETRY OF THE WEST SEGMENT OF THE SOUTH DABASHAN FTB

### Detachment Layers

We identified three of the most important sets of detachment layers in the South Dabashan Belt: (1) Middle Triassic Jialingjiang

Formation gypsum interval, (2) Lower Silurian mudstone zone, and (3) Lower Cambrian shale bed, using a field geological survey, drill core observations, and seismic profile analysis.

In the study area, the thick-bedded gray-white gypsum interval occurs in the Lower Triassic Jialingjiang Formation T1j<sup>4</sup> and T1j<sup>2</sup> members, while dark greenish-gray shale and dark carbonaceous shale occurs in the Lower Silurian and Lower Cambrian areas (**Figure 2**). The gypsum rock, mud, and shale demonstrate the characteristics of plastic flow upon subjection to compression deformation, which is easily transformed into a detachment layer, while the rock strata dominated by limestone and dolomite are mainly characterized by brittle fracture (**Figures 3, 4**).

On the seismic profile, the detachment layer exhibits chaotic or weak seismic event features, and the faults commonly terminate at this layer, resulting in inconsistent deformation of the upper and lower strata (**Figure 3**). In the west segment of the South Dabashan FTB, the Jialingjiang Formation gypsum detachment layer exhibits disordered reflection, and the thickness of deformed strata varies from 100 to 1,500 m (**Figures 5–8**). This can be determined by tracking the top and bottom of the chaotic seismic reflection configuration (**Figure 3A**). The Silurian mudstone and shale detachment layer can be clearly observed in the seismic profiles due to the relatively low amplitude of the seismic event of the overlying and underlying strata, and faults are often developed along the detachment layer (**Figure 3B**). The Cambrian detachment layer exhibits strong reflection in the study area. Unlike the strong fold deformation of the overlying strata, the Cambrian detachment layer is weakly deformed (**Figure 3C**).

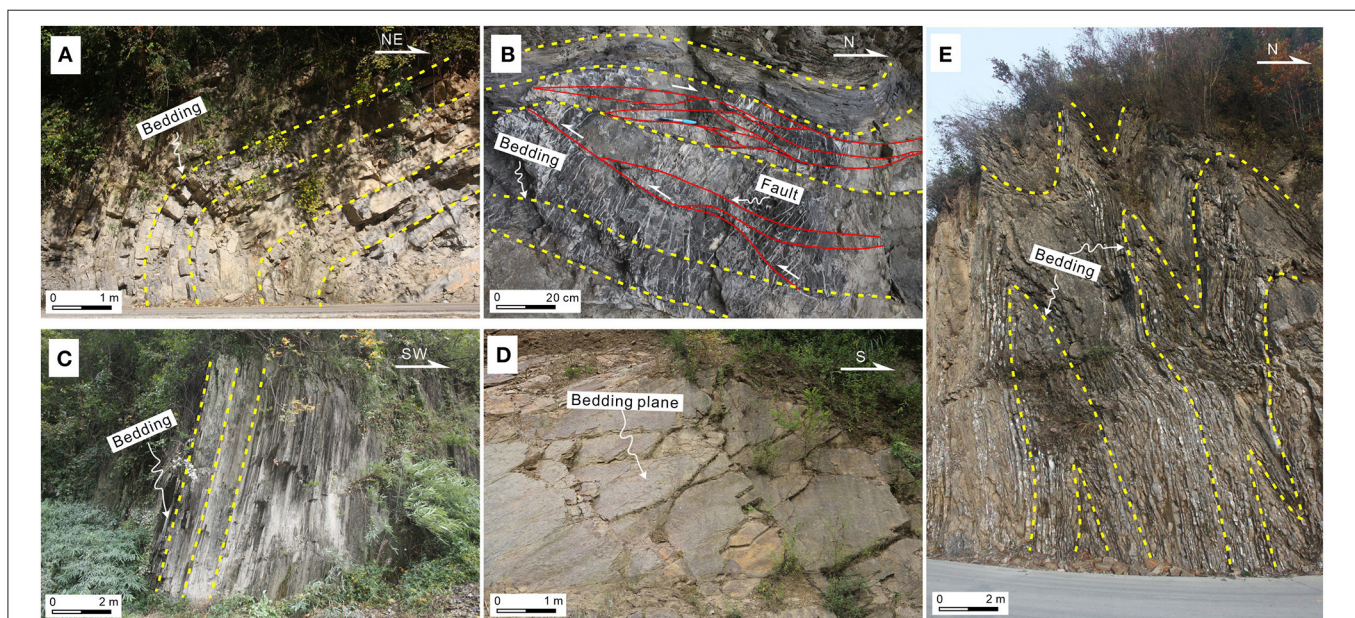
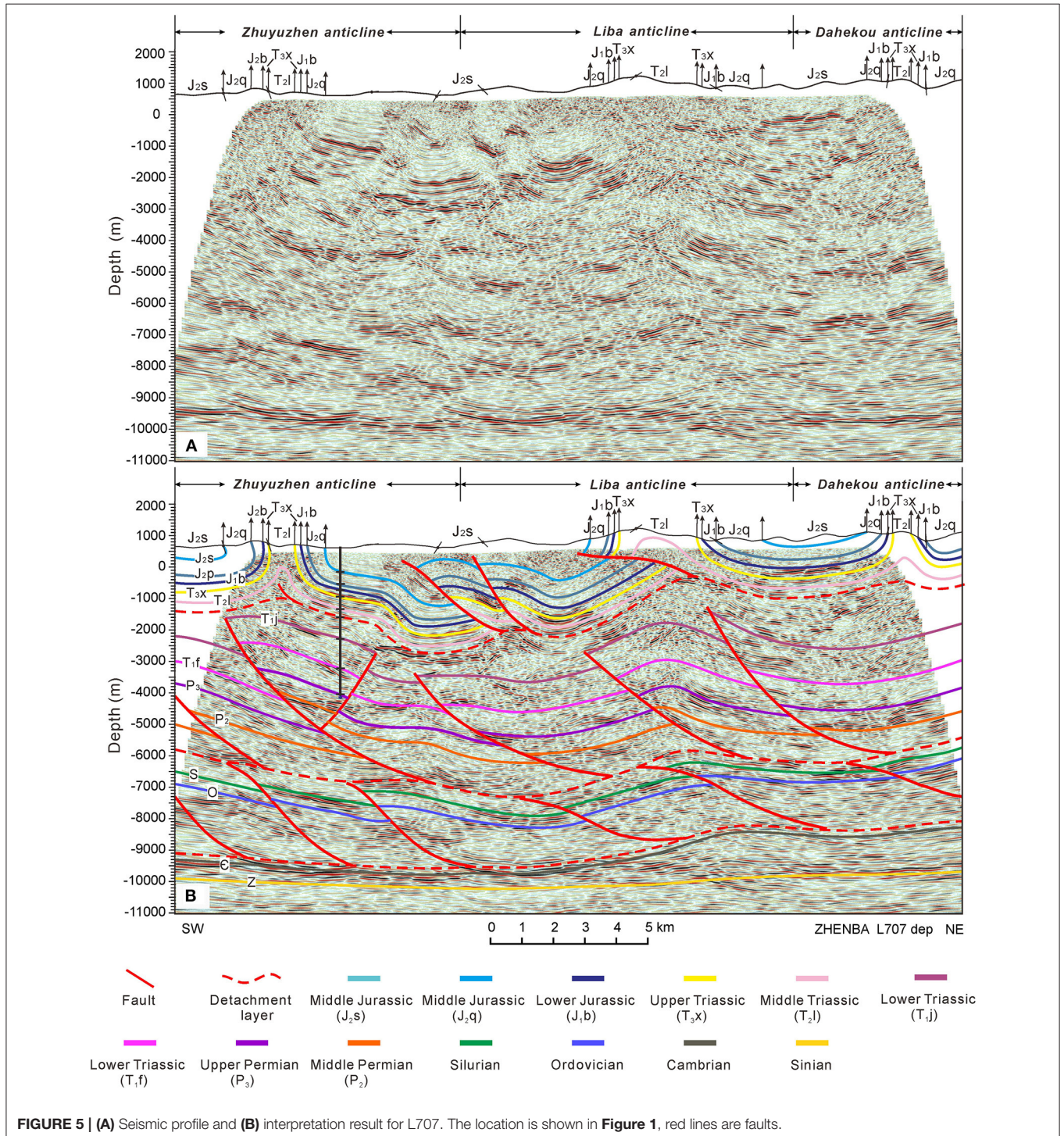


**FIGURE 4 |** Outcrops photographs of the detachment layers. **(A)** An inclined fold with a vertical-to-overturned forelimb, Lower Triassic Jialingjiang Formation (N 32°16'24.1", E 107°56'58.8"). **(B)** An inverted limb of a recumbent fold, Lower Triassic Jialingjiang Formation (N 32°16'24.2", E 107°56'58.8"). **(C)** Thin-bedded mudstone, a part of fold limb with high dip angle, Lower Silurian (N 32°16'34.1", E 108°7'15.5"). **(D)** Mudstone sliding surface, Lower Silurian (N 32°9'50.7", E 108°11'42.3"). **(E)** Steeply inclined folds characterized by a chevron geometry, Lower Cambrian (N 32°17'28.4", E 108°3'38.8").

On the outcrop scale, the detachment layer is characterized by cataclasites, small folds, and well-developed small faults (Figure 4). In addition, folds are typically recumbent or overturned (Figures 4A,E). In the Dabashan area, inclined fold and interlayer-gliding structures of the Jialingjiang Formation are often observed (Figures 4A,B). The mudstone and shale of the Lower Silurian are characterized by a rich sliding

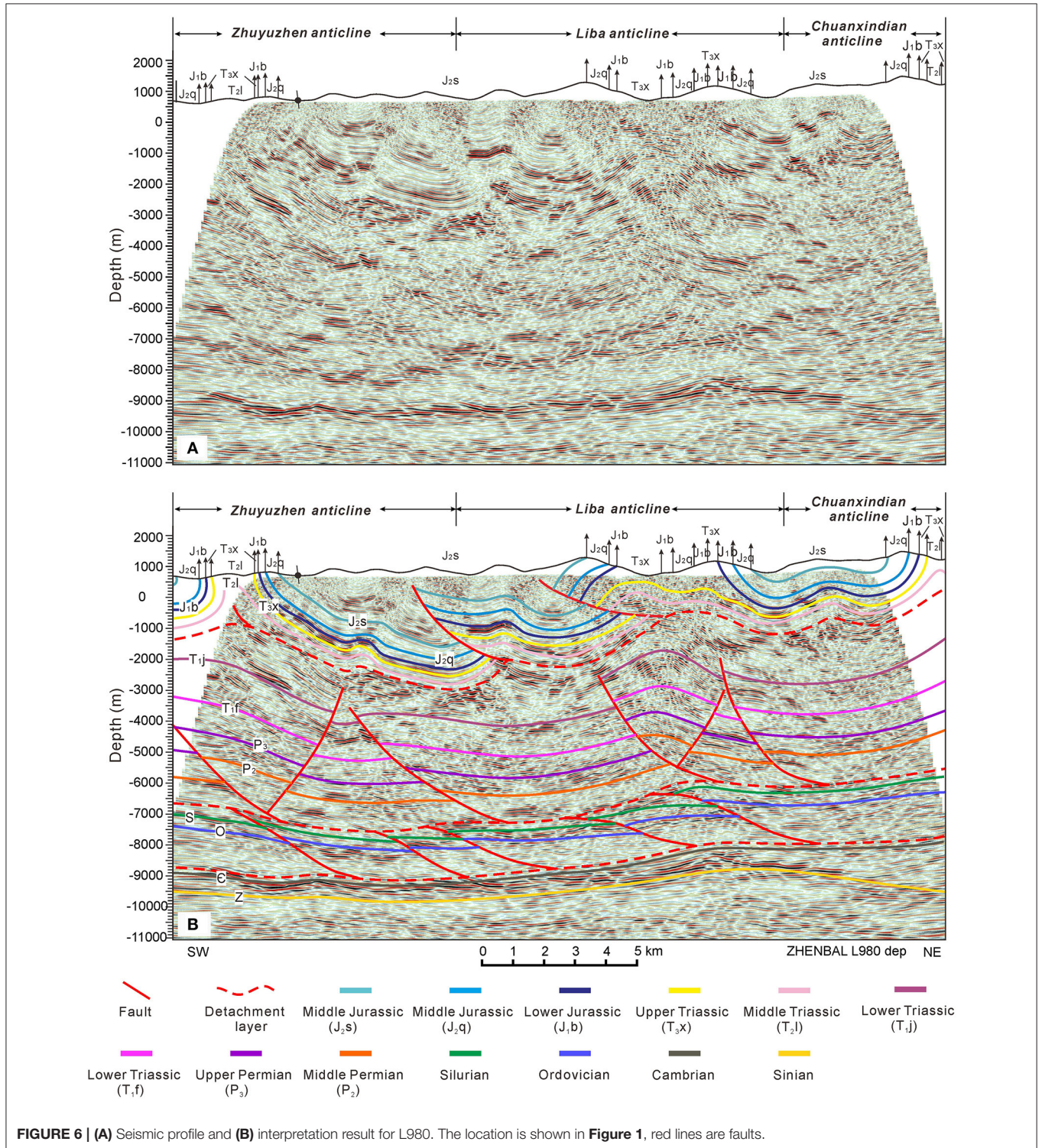
surface (Figures 4C,D). A large number of polyharmonic folds are developed in the Lower Cambrian mudstone and shale (Figure 4E).

According to the above-mentioned analysis, the gypsum strata of the Lower Triassic Jialingjiang Formation, Silurian mudstone, and Cambrian shale exhibited the characteristics of detachment. The South Dabashan Belt exhibits structural



characteristics of multi-level deformation features due to the effect of these sets of detachment layers. Considering the detachment layer as the boundary, the study area can be

divided into the upper structural deformation system, the middle structural deformation system, and the lower structural deformation system.



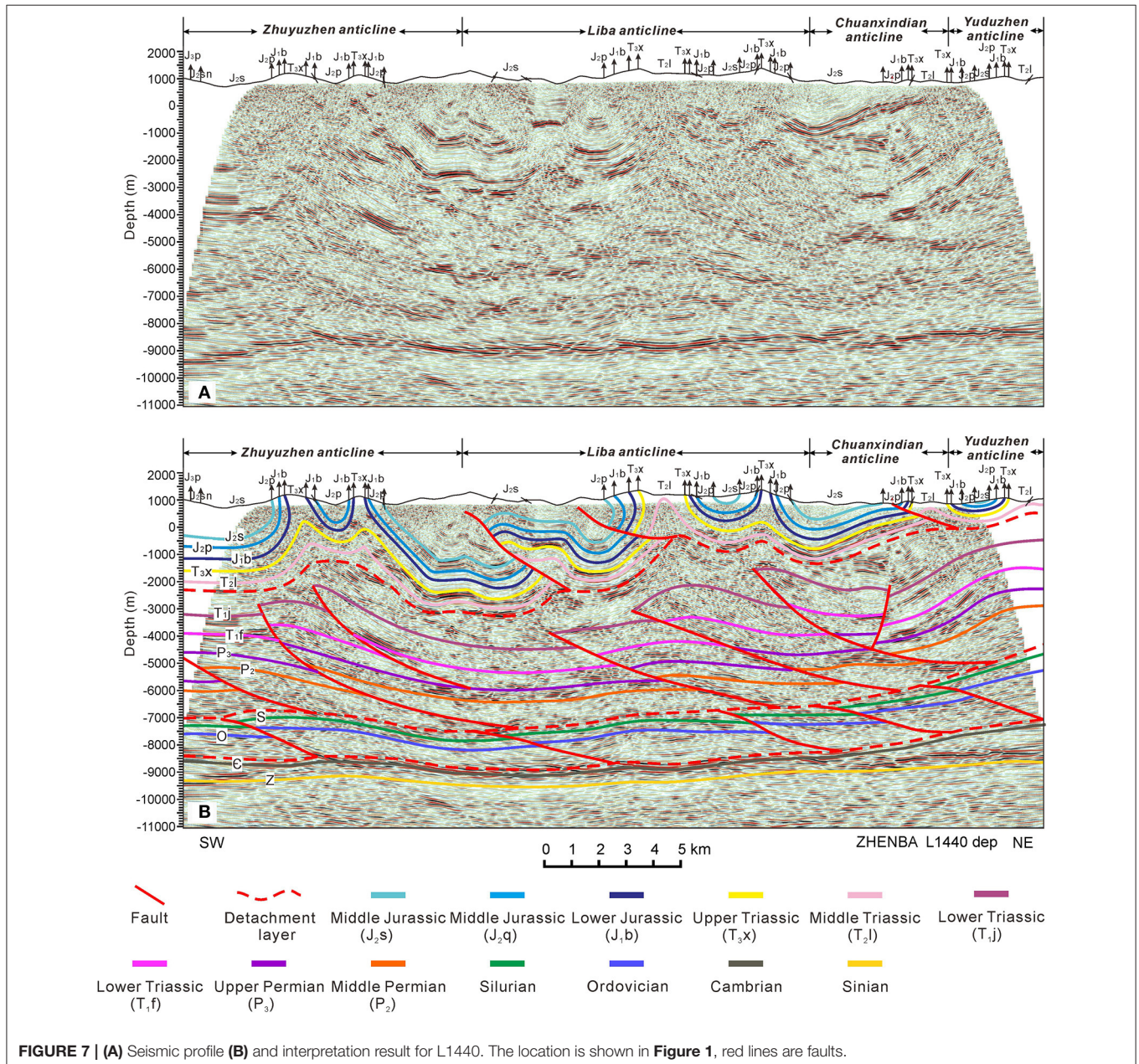


## Structural Geometric Feature of the West Segment of South Dabashan

### Structural Geometric Feature of the South Dabashan Belt

Three 3D seismic profiles were selected to conduct structural interpretation. The seismic profile Zhenba L707 goes through the well ZY-1. Based on the synthetic seismogram of this well, in the Xujiache Formation, the strong reflection seismic horizons of the upper structural deformation system were identifiable. From the original seismic profile (Figure 5A), the maximum buried depth of the Xujiache Formation can reach below 2,000 m above sea level, while the shallowest depth is exposed at the

surface, with a height difference that exceeds 3,000 m. The two limbs of the Zhuyuzhen and Liba anticlines are almost upright and partially split by thrust faults, indicating that the upper structural deformation system in this area has strong tectonic deformation. A series of synclines and anticlines demonstrate that a typical Jura-fold belt style was developed. The development of a structural wedge and back-fault complicates the structural deformation of the upper structural deformation system. There are three anticline structures, namely, Zhuyuzhen, Liba, and Dahekou anticlines from the southwest to the northeast. The core of the anticline is narrow and mainly exposed to Lower-to-Middle Triassic strata. Two wide (5–10 km) synclines are



sandwiched between the three anticlines, while the syncline between the Zhuyuzhen anticline and the Liba anticline is split by faults, forming secondary anticlines and synclines. This indicates that the NE–SW-trending tectonic compression occurred again after the formation of the main fold, which resulted in the stratigraphic offset of the upper structural deformation system. Generally, these synclines and anticlines are gradually uplifted from the southwest to the northeast under the control of a series of thrust faults that developed in the detachment layer with different depths (Figure 5B).

The middle structural deformation system is generally characterized by weak reflection on seismic profiles, whereas the bottom of the Upper Permian is characterized by strong reflection. The seismic horizons are discontinuous, truncated, and overlapped. Several up-steep and down-gentle thrust faults that exit upward in the gypsum bed of the Jialingjiang Formation and converge downward at the Silurian bottom surface are developed in the middle structural deformation system. These faults are superimposed longitudinally to form the imbricate structure style. Under the Zhuyuzhen and Liba anticlines, several fault-related anticlines developed in the middle structural deformation system, causing the upper structural deformation system to sharply rise.

In the lower structural deformation system, the Silurian bottom is characterized by strong reflection, along with the truncation and overlapping of discontinuous seismic horizons. Unlike the middle structural deformation system, the stratigraphic overlap of the lower structural deformation system mainly occurs near the northeast side, and the seismic horizon of the Cambrian bottom is continuous and parallel. A series of low-dipping to subhorizontal thrust faults is developed in the deep structural deformation system, which has an overlying Silurian shale detachment layer as the roof fault and the underlying Cambrian shale detachment layer as the floor fault, forming a duplex structure. The thrust faults in the deep and middle deformation systems reveal different geometries and orientations, and the faults in the lower structural deformation system often turn forward, providing the dip angle of the faults their up-gentle and down-steep features. The shortening of strata is concentrated in the northeast and gradually decreases toward the Sichuan Basin. The Sinian and Proterozoic strata under the Cambrian detachment are generally distributed horizontally, and do not participate in deformation (Figure 5B).

Despite the similarity of the interpreted structural models of L980 and L1440 seismic profiles to L707, some differences were observed (Figures 6, 7). In the upper structural deformation

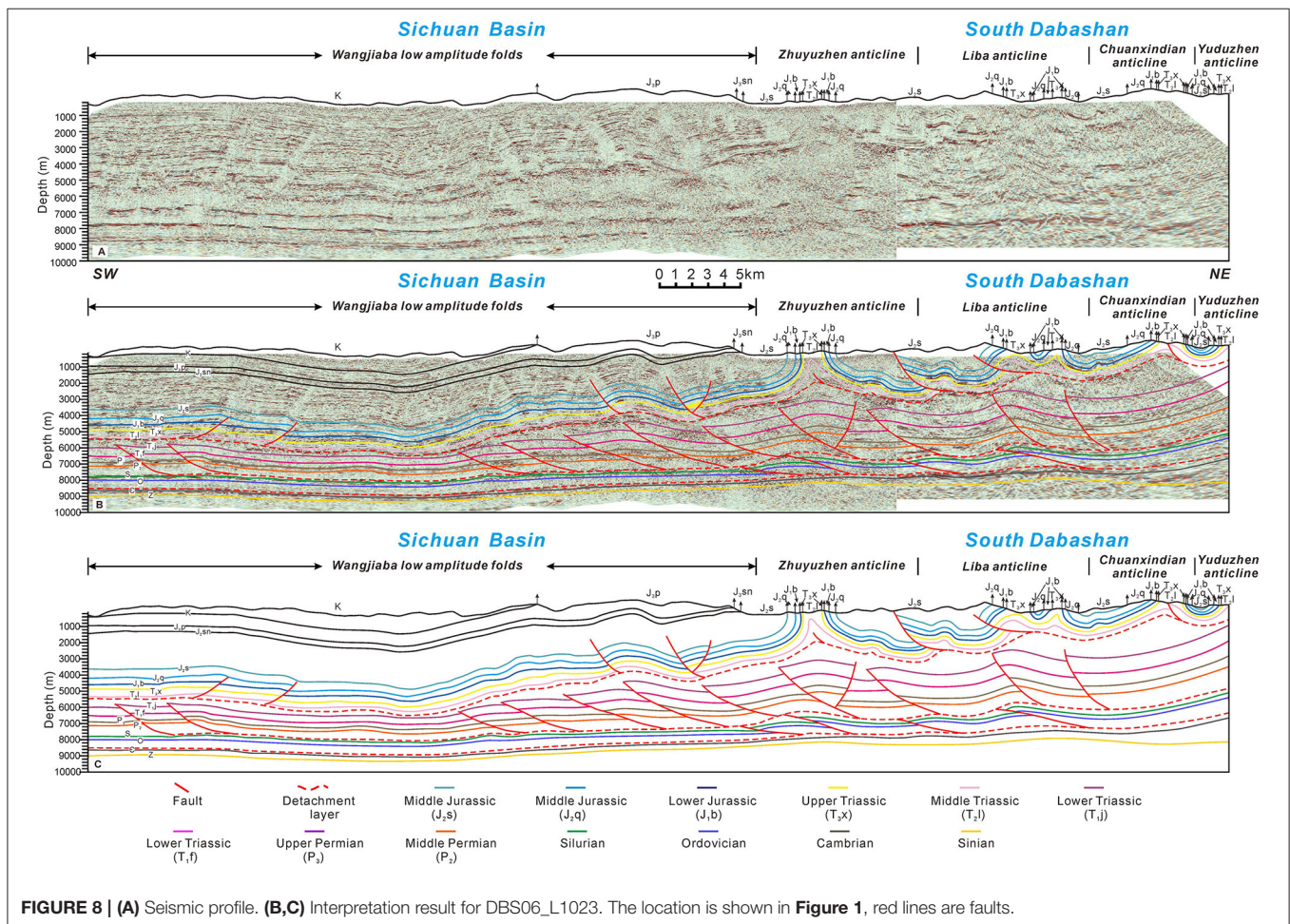


FIGURE 8 | (A) Seismic profile. (B,C) Interpretation result for DBS06\_L1023. The location is shown in Figure 1, red lines are faults.

system, the Zhuyuzhen anticline in the L980 seismic profile is reversed, and the anticline in the L1440 seismic profile is further divided into two small anticlines. The Liba anticline is also transformed into two small anticlines in the L980 and L1440 profiles. In the middle structural deformation system, profile L1440 slightly varies from the two other profiles; the dip angle of the fault is smaller, but the fault displacement is larger under the Liba anticline, which further enlarges the structural amplitude of the Liba anticline. The structural styles of the deep structural layers of the three seismic profiles underwent little change, and are all characterized by imbricate faults tending toward the northeast.

### Structural Geometric Feature of the South Dabashan Belt and the Sichuan Basin

The tectonic deformation characteristics across the South Dabashan Belt and the northern Sichuan Basin were obtained by stitching the 2D and 3D seismic profiles together (Figure 8). The upper structural deformation system in the northern Sichuan Basin is characterized by the Wangjiaba low-amplitude fold belt and the tectonic deformation intensity is weak, while several fault-related folds developed with strong tectonic deformation in the South Dabashan Belt. A large number of imbricated structures are developed in the middle structural deformation system of the South Dabashan Belt, but the number of thrust faults decreases rapidly toward the Sichuan Basin, and the deformation intensity weakens. The deep structural deformation system in the Southern Dabashan Belt has the Cambrian detachment layer as the floor fault and the Silurian detachment layer as the roof fault, forming a duplex structure, but it only extends below the Zhuyuzhen anticline, and the

structural deformation system in the Sichuan Basin exhibits no significant deformation.

Tectonic restoration was conducted in the afore-mentioned section (Figure 9). Considering the three detachment layers as the boundary, the shortening rates of the three structural layers were different, indicating the characteristics of multi-level detachment deformation in this area. The shortening distance of the upper, middle, and lower structural deformation systems were obtained as 7.98, 6.00, and 4.25 km, respectively (Figure 9).

### Features of the Magnetotelluric Profile in the Dabashan Belt

The magnetotelluric profile across the North and South Dabashan Belt and the detachment layer exhibited low resistivity and high conductivity. The magnetotelluric profile shows that the resistivity in the Dabashan area has evident layered characteristics (Figure 10). High-resistivity zones with obvious characteristics are distributed within depths ranging from 0 to 5 km, low resistivity zones within depths ranging from 7 to 28 km, and middle resistivity zones below 28 km. In the North Dabashan Belt, the distribution depth of the high-resistivity zone ranges between 0 and 3 km, which represents the sedimentary cover above the basement. However, the depth of the high-resistivity zone in the South Dabashan Belt ranges from 0 to 5 km, which may represent the stratigraphic unit above the gypsum rock detachment layer of the Jialingjiang Formation, i.e., the Jura-type fold belt in the upper structural deformation system. The vertical depth range of these high-resistivity zones is characterized by gradually increasing the thickness from northeast to southwest, which is the result of differential uplift and denudation of strata caused by tectonic

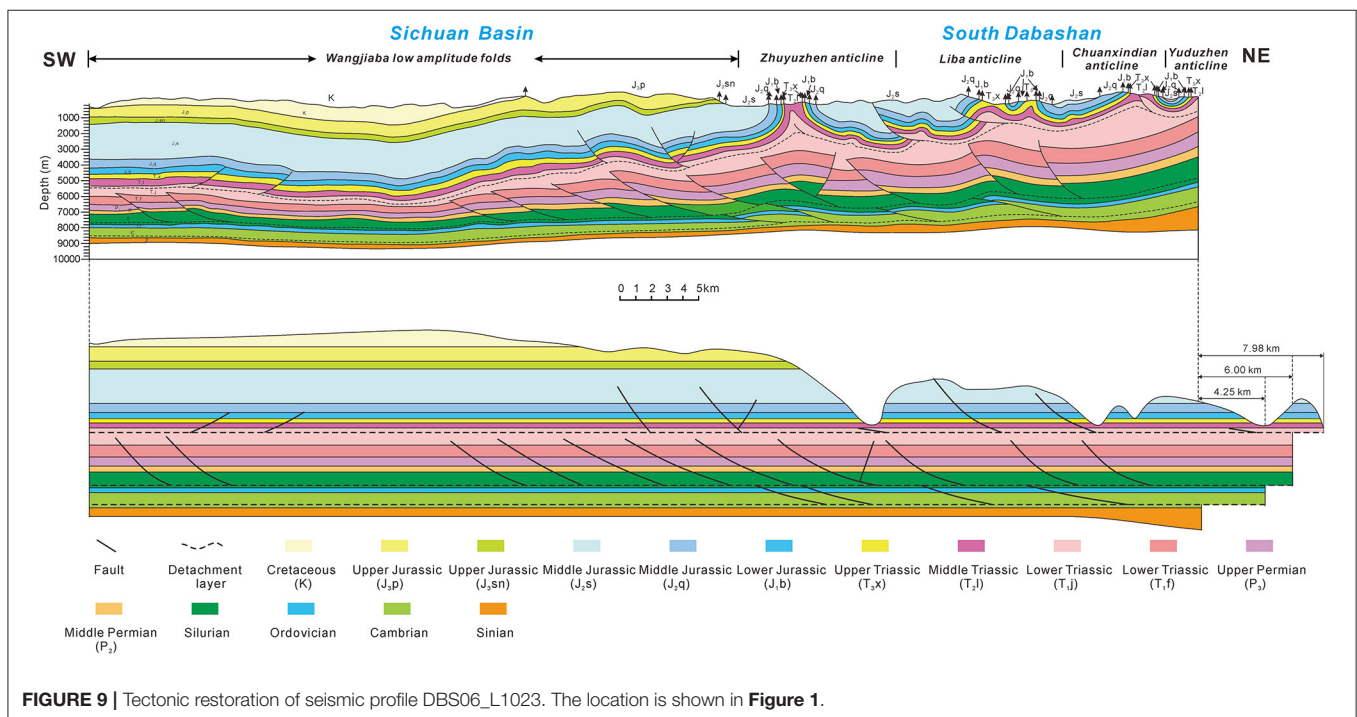
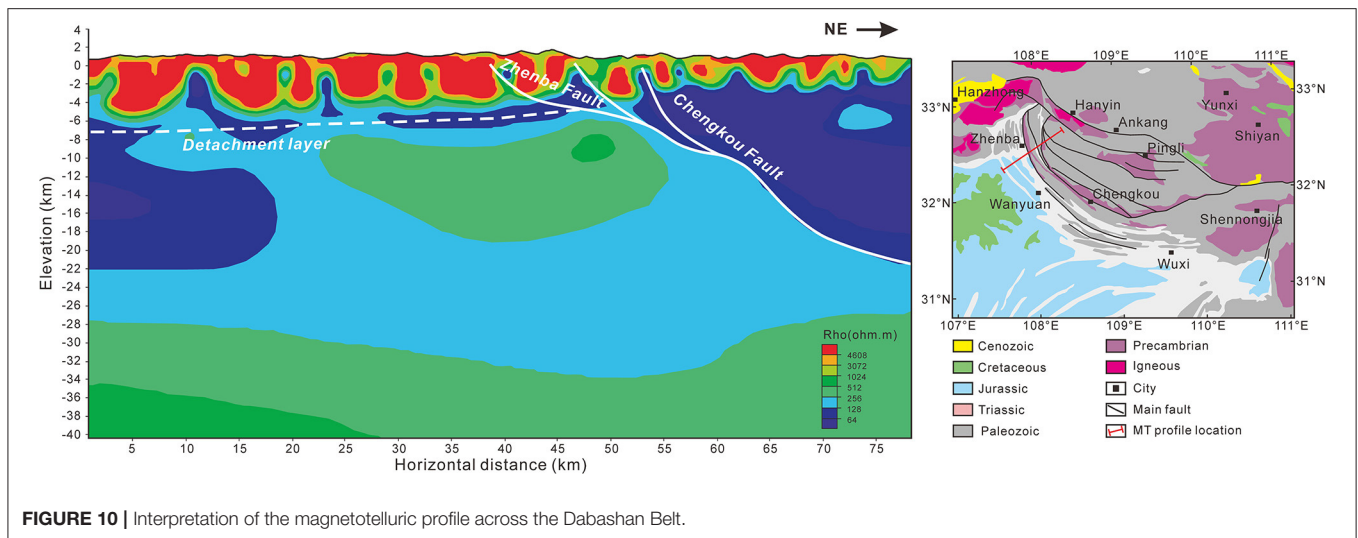


FIGURE 9 | Tectonic restoration of seismic profile DBS06\_L1023. The location is shown in Figure 1.



**FIGURE 10 |** Interpretation of the magnetotelluric profile across the Dabashan Belt.

movement. A low-resistivity zone is evident at 5–7 km under the South Dabashan Belt, which is consistent with the development depth of the Silurian detachment layer identified from the seismic profile. However, the Lower Cambrian detachment layer is relatively thin and no clear response was observed in the magnetotelluric profile. The resistivity distributed in the depth ranging from 7 to 28 km varies greatly but is generally characterized by low resistivity, especially in the North Dabashan Belt in the northeast of the profile, where a wedge-shaped low-resistivity zone can be observed. The lower section of the South Dabashan Belt exhibits a wide range of medium resistivity and has a downward subduction and reduction trend, which may indicate that the South Qinling Belt is pressed and lifted to the southwest, forming a large thrust nappe belt, while the South Dabashan Belt, which belongs to the northern margin of the YZB, subducts downward with the YZB, forming a series of fold-and-thrust belts in the shallow section. There are several resistivity anomaly zones in the middle of the profile, which may be caused by the upward intrusion of deep magma, while the low-resistivity zone at a depth of 10–22 km in the southwest of the profile may correspond to the pre-Sinian ductile shear layer, although the detachment layer has little influence on the tectonic deformation of the west segment of the South Dabashan FTB.

## DISCUSSION

### Structural Kinematic of the West Segment of the South Dabashan FTB

The formation of the North Dabashan Belt was closely related to the collision orogeny between the NCB and SCB in the late Indosinian period, whereas the formation of the South Dabashan arcuate belt was mainly related to the intracontinental orogeny after the collision (Shi et al., 2012, 2013). The uplift and denudation process of the South Dabashan Belt and its adjacent areas have been extensively researched (Yue, 1998; Wang et al.,

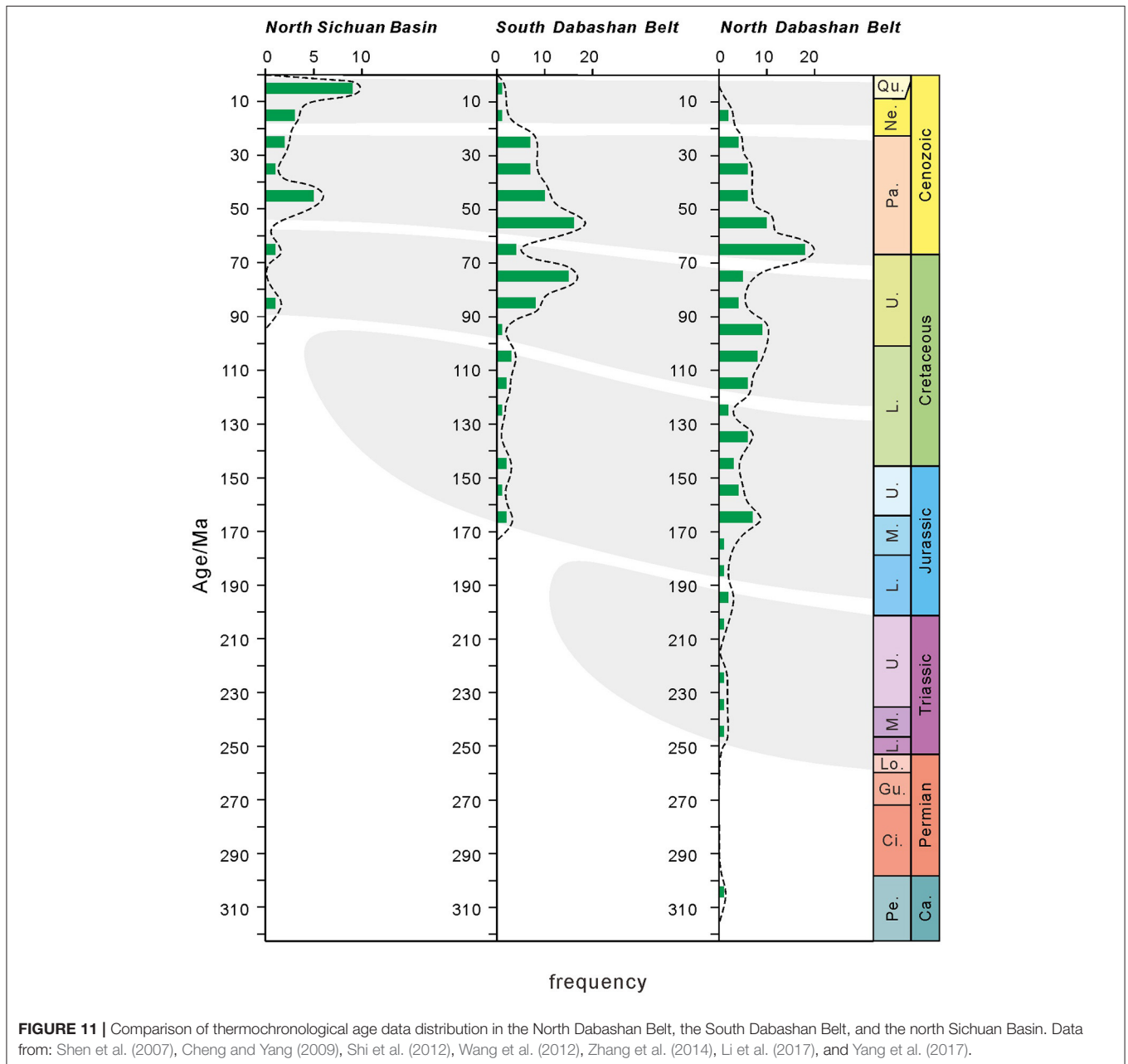
2004; Li et al., 2012; Deng et al., 2013). The low-temperature thermochronological data demonstrate that the uplift age of the strata from the North Dabashan Belt to the Sichuan Basin decreases gradually (Ratschbacher et al., 2003; Shen et al., 2007, 2008; Cheng and Yang, 2009; Li J. et al., 2010; Li P. Y. et al., 2010; Xu et al., 2010; Yang et al., 2017), showing the characteristics of forward expansion deformation. In combination with previous research results (Shen et al., 2007; Cheng and Yang, 2009; Shi et al., 2012; Wang et al., 2012; Zhang et al., 2014; Li et al., 2017; Yang et al., 2017), we divided the tectonic evolutionary history of the study area into four stages (**Figure 11**): Late Jurassic to Early Cretaceous, Late Cretaceous, Paleogene, Neogene to Quaternary. Combined with the previous analysis of geological structure, deformation style, and deformation time in the southern Dabashan area, we established a possible tectonic evolution model.

### Late Jurassic to Early Cretaceous

Under the influence of the Yanshanian movement, the North Dabashan nappe tectonic belt was strongly squeezed and advanced to the northern margin of the YZB, resulting in the earliest deformation on the northeastern margin of the South Dabashan Belt. Among them, thrust faults were developed in the middle and lower structural deformation system, leading to the passive uplift of the overlying strata. The upper structural deformation system mainly developed the low-amplitude fold related to the faults with small fault displacement (**Figure 12**).

### Late Cretaceous

The tectonic deformation of the South Dabashan Belt was further intensified. The imbricated tectonic wedge was formed in the deep structural deformation system, leading to the uplift of the overlying strata. Due to the effect of the detachment layer, the stacking anticlines were formed in the middle and upper structural deformation systems (**Figure 12**).



### Paleogene

The structural deformation of the South Dabashan Belt was further transmitted to the southwest, the main faults in the study area were essentially formed, the embryonic folding of the Zhuyuzhen anticline at the front was formed, and the deformation of the middle structural deformation system was complicated under the control of fault deformation (Figure 12).

### Neogene to Quaternary

Influenced by the Himalayan movement, the South Dabashan Belt rose and suffered denudation. Little change was observed in the deep structural layers, but the fault displacement and structural amplitude of the middle and upper structural

deformation systems significantly increased. The fault plane was deformed, and some back-faults were formed in the upper structural deformation system, and the strata on both wings of the folds became steeper (Figure 12).

### Implication for the Multi-Level Detachment Deformation

The new deep seismic profile data provide evidence for the intracontinental subduction orogenic model in the Dabashan area (Dong et al., 2013). The mafic lower crust subducted below 30 km changed from granulite to eclogite, and the increments in its density and gravity have been used to explain the main driving force of the continuous downward subduction of the YZB. Based

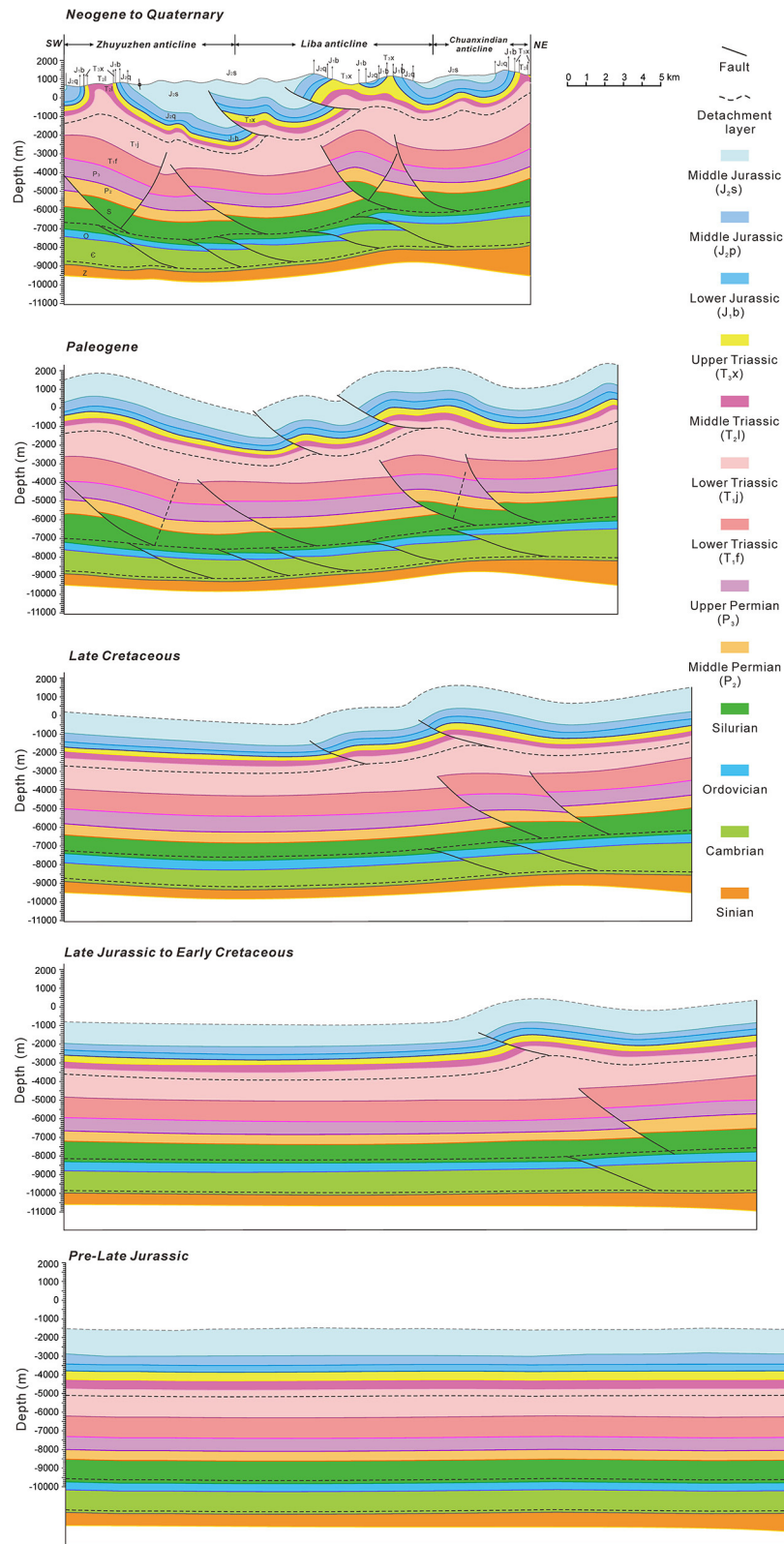
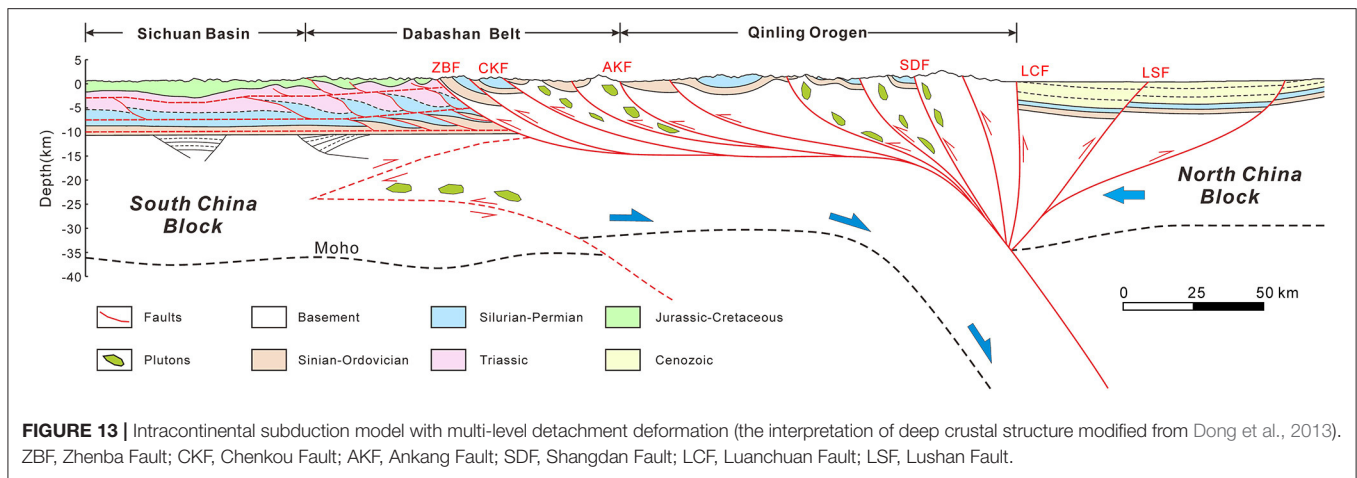


**FIGURE 12 |** Tectonic evolution of the South Dabashan Belt based on interpretation results of the profile line 980.



on the above seismic interpretation results and magnetotelluric data, we present the tectonic deformation model of the Qinling Orogenic Belt and the northern margin of the YZB, focusing on the relationship between the tectonic deformation pattern in the Southern Dabashan area and the intracontinental subduction orogenic processes of the YZB and the Qinling Orogenic Belt (**Figure 13**).

Previous analyses of the tectonic stress field in the South Dabashan fold-and-thrust belt revealed that the main tectonic stress stems from the Qinling Orogenic Belt (Li et al., 2005, 2006; Liu et al., 2005), and its stress field bears the characteristics of multiple superpositions (Shi et al., 2012, 2013). The bidirectional Qinling Orogenic Belt was formed by the collision and combination of the NCB and SCB during the late Indosinian period (Xu et al., 1986; Meng and Zhang, 1999; Xiao et al., 2011). From the Early Triassic to the Middle Jurassic, the North Dabashan thrust nappe structural belt began to form gradually in the passive continental margin near the YZB (Zhang et al., 2010; Shi et al., 2012). Since the Late Jurassic, the North Dabashan Belt has been continuously compressed to the southwest, leading to further intracontinental structural deformation in the South Dabashan Belt, forming an arcuate fold-and-thrust belt. However, the North Dabashan Belt and the South Dabashan Belt belong to different blocks, and the CKF was a regional normal fault in a passive continental margin setting for a long time during the Paleozoic, which controlled the basin boundary and sedimentary environment (Li J. et al., 2018). Therefore, in the later stage of intracontinental orogeny, the CKF reversed and became a high-angle reverse fault, forming the boundary between the North Dabashan Belt and the South Dabashan Belt. The South Dabashan Belt was not involved in the thrust nappe tectonic system of the North Dabashan Belt during the intracontinental orogeny because of the separation of the South Dabashan Belt and the North Dabashan Belt by the CKF, and the multi-layered stratigraphic units of the South Dabashan Belt.

Multiple sets of detachment layers developed in the northern margin of the YZB formed three main structural deformation systems with different depths during the intracontinental

orogeny processes in the South Dabashan FTB. Due to the partition effect of the detachment layers, each structural deformation system is not coupled, and their shortening of formations gradually increases from top to bottom. These detachment layers absorb the displacement of the upward propagation of faults, which inhibits the possibility of the integral deformation of the sedimentary cover above the basement, making it impossible to form large faults that cut through the entire sedimentary cover, and the related large thrust nappe structures are difficult to form. Therefore, in the process of regional compressive stress spreading to the southwest, the South Dabashan FTB was influenced by longitudinal heterogeneity stratigraphic combination and formed a multi-level intracontinental detachment deformation style (**Figure 13**).

## CONCLUSIONS

Three main detachment layers developed in the west segment of the South Dabashan FTB: the Jialingjiang Formation gypsum interval, Silurian mudstone beds, and Cambrian shale beds. Controlled by the three detachment layers, the west segment of the South Dabashan FTB forms three structural deformation systems with relatively independent structural styles at different depths. The upper structural deformation system is characterized by Jura-style folds, the imbricate thrusts developed in the middle structural deformation system; and the lower structural deformation system is controlled by the duplex structure.

At different depths, the detachment layer absorbs most of the fault displacement, which results in each structural deformation system having a relatively independent structural style. The shortening of the deep structural deformation system has the smallest, followed by the middle which is larger, and finally, the upper structural deformation system has the largest structural shortening. This may be caused by differences in strain partitioning between varying structural deformation systems under the control of different slip layers.

The Southern Dabashan arcuate FTB was formed during the subduction of the YZB under the NCB, and the regional compressive stress from the Qinling Orogenic Belt controlled

the propagation deformation process in the Dabashan area. The regional boundary fault and the longitudinal heterogeneous stratigraphic combination both control the tectonic deformation process of the South Dabashan Belt, giving it the intracontinental orogeny style of multi-level slip deformation.

This study combines surface data and seismic data to establish a more accurate structural model in the study area. However, due to the limitations of geophysical technology and complicated geological structure conditions in South Dabashan, the imaging effect of the current seismic profile may be affected, thus the real underground structure cannot be described in detail. Thus, the optimization of seismic acquisition and processing technology, in conjunction with more detailed fieldwork is required in the future to improve our understanding.

## DATA AVAILABILITY STATEMENT

The original contributions presented in the study are included in the article/**Supplementary Material**, further inquiries can be directed to the corresponding author/s.

## AUTHOR CONTRIBUTIONS

HH and QM initiated the study, carried out seismic interpretations, and wrote the manuscript. DH developed

the project idea and secured financial support. QM and YL participated in the collection of seismic data. RL and YL provided helpful discussions and helped to improve the manuscript. All authors contributed to the article and approved the submitted version.

## FUNDING

This research was financially supported by the National Science and Technology Major Project (2017ZX05001), the National Natural Science Foundation of China (41430316), and the National Key R&D Program of China (2017YFC0601405).

## ACKNOWLEDGMENTS

We thank Sinopec Exploration Southern Company for kindly supplying drilling and seismic data. We also thank Longbo Chen, Zhu Wen, and Li Zhang for their help in carrying out the fieldwork.

## SUPPLEMENTARY MATERIAL

The Supplementary Material for this article can be found online at: <https://www.frontiersin.org/articles/10.3389/feart.2021.633816/full#supplementary-material>

## REFERENCES

- Cheng, W. Q., and Yang, K. G. (2009). Structural evolution of Dabashan Mountain: evidence from ESR dating. *Earth Sci. Front.* 16, 197–206. doi: 10.1016/S1874-8651(10)60080-4
- Dahlstrom, C. D. A. (1969). Balanced cross sections. *Can. J. Earth Sci.* 6, 743–757. doi: 10.1139/e69-069
- Dean, S., Morgan, J., and Brandenburg, J. P. (2015). Influence of mobile shale on thrust faults: Insights from discrete element simulations: influence of Mobile Shale on Thrust Faults. *AAPG Bull.* 99, 403–432. doi: 10.1306/10081414003
- Deng, B., Liu, S. G., Li, Z. W., Jansa, L. F., Liu, S., Wang, G. Z., et al. (2013). Differential exhumation at eastern margin of the Tibetan Plateau, from apatite fission-track thermochronology. *Tectonophysics* 591, 98–115. doi: 10.1016/j.tecto.2012.11.012
- Deng, B., Liu, S. G., Liu, S., Li, Z. W., Si, J. T., Guo, B., et al. (2010). The structural features of Jiaochang Arc Belt in Songpan-Ganzi Fold Belt and its tectonic implications. *Geol. Rev.* 56, 31–42.
- Dong, S., Gao, R., Yin, A., Guo, T., Zhang, Y., Hu, J., et al. (2013). What drove continued continent-continent convergence after ocean closure? Insights from high-resolution seismic-reflection profiling across the Daba Shan in central China. *Geology* 41, 671–674. doi: 10.1130/G34161.1
- Dong, Y., Liu, X., Zhang, G., Chen, Q., Zhang, X., Li, W., et al. (2012). Triassic diorites and granitoids in the Foping area: constraints on the conversion from subduction to collision in the Qinling orogen, China. *J. Asian Earth Sci.* 47, 123–142. doi: 10.1016/j.jseas.2011.06.005
- Dong, Y. P., Shen, Z. Y., Xiao, A. C., Wang, L., Mao, L. G., and Wei, G. Q. (2011). Construction and structural analysis of regional geological sections of the southern Daba Shan thrust-fold belts. *Acta Petrol. Sin.* 27, 689–698.
- Dong, Y. P., Zha, X. F., Fu, M. Q., Zhang, Q., Yang, Z., and Zhang, Y. (2008). Characteristics of the Dabashan fold and thrust nappe structure at the southern margin of the Qinling, China. *Geol. Bull. China* 27, 1493–1508. doi: 10.1163/ej.9789004122550.i-610.106
- Geiser, P. A. (1988). The role of kinematics in the construction and analysis of geological cross sections in deformed terranes. *Geometr. Mech. Thrust.* 222, 47–76. doi: 10.1130/SPE222-p47
- He, J. K., Lu, H. F., Zhang, Q. L., and Zhu, B. (1997). The thrust tectonics and its transpressive geodynamics in southern Dabashan Mountains. *Geol. J. China Univers.* 3, 419–428.
- Huang, H., He, D., Li, D., and Li, Y. (2020). Detrital zircon U-Pb ages of Paleogene deposits in the southwestern Sichuan foreland basin, China: constraints on basin-mountain evolution along the southeastern margin of the Tibetan Plateau. *Geol. Soc. Am. Bull.* 132, 668–686. doi: 10.1130/B35211.1
- Huang, H., He, D., Li, Y., Li, J., and Zhang, L. (2018). Silurian tectonic-sedimentary setting and basin evolution in the Sichuan area, southwest China: implications for palaeogeographic reconstructions. *Mar. Petroleum Geol.* 92, 403–423. doi: 10.1016/j.marpetgeo.2017.11.006
- Lai, S., Zhang, G., Dong, Y., Pei, X. Z., and Chen, L. (2004). Geochemistry and regional distribution of ophiolites and associated volcanics in Mianlue suture, Qinling-Dabie Mountains. *Sci. China Ser. D Earth Sci. English Edn.* 47, 289–299. doi: 10.1360/02YD0474
- Lai, S., Zhang, G., and Yang, R. (2000). Identification of the island-arc magmatic zone in the Lianghe-Raofeng-Wuliba area, south Qinling and its tectonic significance. *Sci. China Ser. D Earth Sci. English Edn.* 43, 69–81. doi: 10.1007/BF02911934
- Li, J., Li, Z., Liu, S., Ran, B., Ye, Y., Deng, B., et al. (2018). Kinematics of the Chengkou fault in the south Qinling orogen, Central China. *J. Struct. Geol.* 114, 64–75. doi: 10.1016/j.jsg.2018.06.008
- Li, J., Zhang, Y., Dong, S., Shi, W., Li, H., Li, J., et al. (2010). Apatite fission track thermochronologic constraint on Late Mesozoic uplifting of the Fenghuangshan basement uplift. *Dizhi Kexue/Chin. J. Geol.* 45, 969–986. doi: 10.3969/j.issn.0563-5020.2010.04.004
- Li, P. Y., Zhang, J. J., Guo, L., and Yang, X. Y. (2010). Structural features and deformational ages in the front of the northern Dabashan thrust belt. *Earth Sci. Front.* 17, 191–199.



- Li, W., Liu, S., Wang, Y., Qian, T., and Gao, T. (2017). Duplex thrusting in the South Dabashan arcuate belt, central China. *J. Struct. Geol.* 103, 120–136. doi: 10.1016/j.jsg.2017.09.007
- Li, Y., He, D., Li, D., Lu, R., Fan, C., Sun, Y., and Huang, H. (2018). Sedimentary provenance constraints on the Jurassic to Cretaceous paleogeography of Sichuan Basin, SW China. *Gondwana Res.* 60, 15–33. doi: 10.1016/j.gr.2018.03.015
- Li, Z., Liu, S., Luo, Y., Liu, S., and Xu, G. (2006). Structural style and deformational mechanism of southern Dabashan foreland fold and thrust belt in central China. *Geotectonica et Metallogenia* 30, 294–304. doi: 10.1007/s11442-006-0415-5
- Li, Z. K., and Ding, Y. Y. (2007). A tentative discussion on characteristics of the Daba Mountain nappe structure. *Geophys. Geochem. Explor.* 31, 495–498. doi: 10.3969/j.issn.1000-8918.2007.06.004
- Li, Z. W., Liu, S., Chen, H., Deng, B., Hou, M., Wu, W., et al. (2012). Spatial variation in Meso-Cenozoic exhumation history of the Longmen Shan thrust belt (eastern Tibetan Plateau) and the adjacent western Sichuan basin: constraints from fission track thermochronology. *J. Asian Earth Sci.* 47, 185–203. doi: 10.1016/j.jseas.2011.10.016
- Li, Z. W., Luo, Y.H., Liu, S.G., Shan, Y.M., Liu, W.G., and Liu, S. (2005). Acoustic emission experiment and estimation of tectonic paleostress in reservoir rocks of upper Triassic and Jurassic, the northeast of Sichuan, China. *J. Chengdu Univ. Technol.* 32, 614–620 (in Chinese with English abstract). doi: 10.1016/j.jcv.2015.07.190v
- Liu, S., Li, W., Wang, K., Qian, T., and Jiang, C. (2015). Late Mesozoic development of the southern Qinling–Dabieshan foreland fold and thrust belt, Central China, and its role in continent–continent collision. *Tectonophysics* 644, 220–234. doi: 10.1016/j.tecto.2015.01.015
- Liu, S., Liu, S. G., Li, Z. W., Yong, Z. Q., and Sun, W. (2005). Analysis of joints from the Meso-Cenozoic tectonic stress field in the west section of south Dabashan fault-fold belt in China. *J. Chengdu Univ. Technol.* 32, 345–350. doi: 10.3969/j.issn.1671-9727.2005.04.003
- Liu, S., and Zhang, G. (1999). Process of rifting and collision along plate margins of the Qinling orogenic belt and its geodynamics. *Acta Geol. Sin. English Ed.* 73, 275–288. doi: 10.1111/j.1755-6724.1999.tb00836.x
- Meng, Q. R., and Zhang, G. W. (1999). Timing of collision of the North and South China blocks: controversy and reconciliation. *Geology* 27, 123–126. doi: 10.1130/0091-7613(1999)027<0123:TOCOTN>2.3.CO;2
- Meng, Q. R., and Zhang, G. W. (2000). Geologic framework and tectonic evolution of the Qinling orogen, central China. *Tectonophysics* 323, 183–196. doi: 10.1016/S0040-1951(00)00106-2
- Morley, C. K., von Hagke, C., Hansberry, R., Collins, A., Kanitpanyacharoen, W., and King, R. (2018). Review of major shale-dominated detachment and thrust characteristics in the diagenetic zone: part II, rock mechanics and microscopic scale. *Earth Sci. Rev.* 176, 19–50. doi: 10.1016/j.earscirev.2017.09.015
- Ratschbacher, L., Hacker, B. R., Calvert, A., Webb, L. E., Grimmer, J. C., McWilliams, M. O., et al. (2003). Tectonics of the Qinling (Central China): tectonostratigraphy, geochronology, and deformation history. *Tectonophysics* 366, 1–53. doi: 10.1016/S0040-1951(03)00053-2
- Shen, C., Tang, J., Mei, L., and Wu, M. (2008). Geochronology evidences for tectonic deformation of Dabashan Fold and thrust Belt in Central China. *Atomic Energy Sci. Technol.* 42, 574–576.
- Shen, C. B., Mei, L. F., Xu, Z. P., Tang, J. G., and Tian, P. (2007). Fission track thermochronology evidence for Mesozoic-Cenozoic uplifting of Daba Mountain, central China. *Acta Petrol. Sin.* 23, 2901–2910. doi: 10.1631/jzus.2007.B0900
- Shi, W., Li, J., Tian, M., and Wu, G. (2013). Tectonic evolution of the Dabashan orocline, central China: insights from the superposed folds in the eastern Dabashan foreland. *Geosci. Front.* 4, 729–741. doi: 10.1016/j.gsf.2013.01.002
- Shi, W., Zhang, Y., Dong, S., Hu, J., Wiesinger, M., Ratschbacher, L., et al. (2012). Intra-continental Dabashan orocline, southwestern Qinling, central China. *J. Asian Earth Sci.* 46, 20–38. doi: 10.1016/j.jseas.2011.10.005
- Wang, J., Qin, J. Q., Liu, W. H., Tao, C., and Teng, G. E. (2012). Mesozoic tectonics and dynamic thermal history in Yuanba area of northeastern Sichuan Basin: application of (U-Th)/He dating of apatite and zircon. *Petroleum Geol. Exper.* 34, 19–24. doi: 10.1007/s12583-013-0355-9
- Wang, T., Zhang, Z. Q., Wang, X. X., Wang, Y. B., and Zhang, C. L. (2005). Neoproterozoic collisional deformation in the core of the Qinling orogen and its age: constrained by zircon SHRIMP dating of strongly deformed syn-collisional granites and weakly deformed granitic veins. *Acta Geol. Sin.* 79, 220–231. doi: 10.1186/1746-6148-10-43
- Wang, Z. C., Zhao, W. Z., Xu, A. N., Li, D. H., and Cui, Y. (2006). Structure styles and their deformation mechanisms of Dabashan foreland thrust belt in the north of Sichuan basin. *Geoscience* 20, 429–435. doi: 10.3969/j.issn.1000-8527.2006.03.010
- Wang, Z. C., Zou, C. N., Tao, S. Z., Li, J., Wang, S. Q., and Zhao, C. Y. (2004). Analysis on tectonic evolution and exploration potential in Dabashan foreland basin. *Acta Petrol. Sin.* 25, 23–28. doi: 10.7623/syxb200406005
- Xiao, A. C., Wei, G. Q., Shen, Z. Y., Wang, L., Yang, W., and Qian, J. F. (2011). Basin- mountain system and tectonic coupling between Yangtze Block and South Qinling Orogen. *Acta Petrol. Sin.* 30, 601–611.
- Xu, C., Zhou, Z., Chang, Y., and Guillot, F. (2010). Genesis of Daba arcuate structural belt related to adjacent basement upheavals: constraints from Fission-track and (U-Th)/He thermochronology. *Sci. China Earth Sci.* 53, 1634–1646. doi: 10.1007/s11430-010-4112-y
- Xu, Z. Q., Lu, Y. L., Tang, Y. Q., Mattauer, M., Matte, Ph., Malavieille, J., et al. (1986). Deformation characteristics and tectonic evolution of the eastern Qinling orogenic belt. *Acta Geol. Sin.* 3, 237–247. doi: 10.1111/j.1755-6724.1986.mp60003003.x
- Yang, Z., Shen, C., Ratschbacher, L., Enkelmann, E., Jonckheere, R., Wauschkuhn, B., et al. (2017). Sichuan Basin and beyond: eastward foreland growth of the Tibetan Plateau from an integration of Late Cretaceous-Cenozoic fission track and (U-Th)/He ages of the eastern Tibetan Plateau, Qinling, and Daba Shan. *J. Geophys. Res.* 122, 4712–4740. doi: 10.1002/2016JB013751
- Yue, G. Y. (1998). Tectonic characteristics and tectonic evolution of Dabashan orogenic belt and its foreland basin. *J. Mineral. Petrol.* 18, 8–15.
- Zhang, Y. N., Li, R. X., Liu, H. Q., Zhu, R. J., Zhu, D. M., Wang, N., et al. (2014). Mesozoic-Cenozoic tectonic uplift history of Dabashan foreland structure in the northern rim of Sichuan Basin. *J. Earth Sci. Environ.* 36, 230–238. doi: 10.3969/j.issn.1672-6561.2014.01.022
- Zhang, Y. Q., Shi, W., Li, J. H., Wang, R. R., Li, H. L., and Dong, S. W. (2010). Formation mechanism of the Dabashan foreland arc-shaped structural belt. *Acta Geol. Sin.* 84, 1300–1315. doi: 10.1017/S0004972710011772

**Conflict of Interest:** QM and YL were employed by the company Sinopec.

The remaining authors declare that the research was conducted in the absence of any commercial or financial relationships that could be construed as a potential conflict of interest.

Copyright © 2021 Huang, Mei, He, Lu and Li. This is an open-access article distributed under the terms of the Creative Commons Attribution License (CC BY). The use, distribution or reproduction in other forums is permitted, provided the original author(s) and the copyright owner(s) are credited and that the original publication in this journal is cited, in accordance with accepted academic practice. No use, distribution or reproduction is permitted which does not comply with these terms.